Acta Chemica Scandinavica A 31 (1977) 461—468

Absorption and Raman Spectra of the Binary Molten Systems $MnCl_2$-$AlCl_3$ and $MnCl_2$-CsCl

WERNER BUES,* LAILA EL-SAYED** and HARALD A. ØYE

Institutt for uorganisk kjemi, Norges tekniske høgskole, Universitetet i Trondheim, N-7034 Trondheim-NTH, Norway

Molten mixtures of $MnCl_2-AlCl_3$ and $MnCl_2-CsCl$ have been studied by absorption and Raman spectroscopy. The complete concentration range was covered for mixtures with CsCl while high vapour pressures prevented studies above 30 mol % $MnCl_2$ in mixtures with $AlCl_3$. The spectral results are discussed with reference to the decrease in acidity in the series $AlCl_3$-$MnCl_2$-CsCl. $MnCl_2$ is considered to be octahedral in mixtures with $AlCl_3$ and mainly tetrahedral in mixtures with CsCl. The spectral changes in mixtures with CsCl are attributed to increased Cl-bridging with increasing $MnCl_2$-content.

As part of our studies on mixtures of covalent and ionic melts,[1-5] the binary melt systems $MnCl_2$-$AlCl_3$ and $MnCl_2$-CsCl were studied spectrophotometrically. These systems span the transition from the covalent melt $AlCl_3$, through the partly covalent $MnCl_2$, to the completely ionic CsCl melt. As Mn^{2+} is spectroscopically active it is possible to detect changes in Mn^{2+} coordination through the changing environments.

The $MnCl_2$-$AlCl_3$ system has recently attracted interest because of its role in the Toth-process for aluminium production.[6,7] The advantage of this process over the existing Bayer-Hall-Heroult process is that the electrolysis step is avoided, with a possible production cost reduction as well as reducing environmental pollution through elimination of fluorides. The crucial step in the process is the manganothermic reduction of $AlCl_3$:

$$3Mn(s) + 2AlCl_3(l) = 3MnCl_2(l) + 2Al(s) \quad (1)$$

This reaction results in a solution of $MnCl_2$ in molten $AlCl_3$ up to 40 mol %. The present spectroscopic study covers the concentration range which is of importance for the technological process, and the data form the basis of current studies of the process itself in this laboratory.

EXPERIMENTAL

Apparatus. The samples were contained in sealed quartz cells. Optical far U.V. cells (Thermal Syndicate Ltd. Wallsend) with 1 mm pathlength were utilized in the absorption spectroscopic studies of $MnCl_2$-CsCl except for the mixture with $X_{MnCl_2} = 0.01$, for which a 1 cm pathlength cell was used. Due to the high pressures generated in the $MnCl_2$-$AlCl_3$ systems, cell strength was considered more important than perfect optical quality, consequently 1 cm pathlength cells were made from heavy duty square tubings (Thermal Syndicate Ltd., Wallsend). These tubings have rounded off corners which are essential for pressure endurance.

The cells were placed in a Kanthal-wound furnace with three separate heating elements and a "see-through" channel to transmit a light beam. The heating elements were connected to a EUROTHERM (PID) controller, which permitted maintenance of a temperature gradient of less than 2 °C over the sample.

A Cary 17H high-temperature absorption spectrophotometer (Cary Instruments, Monrovia, USA) with an optical range 186 – 2650 nm was used for obtaining the spectra. The

* Anorganisch-Chemisches Institut der Technischen Universität Clausthal, Lehrstuhl B, 3392 Clausthal-Zellerfeld, Bundesrepublik Deutschland.

** Post doctoral fellow. Permanent address: Chemistry Department, Faculty of Science, Alexandria University, Moharem Bay, Alexandria, Egypt.

Cary spectrophotometer was interphased [8] with a Kennedy 1600 Incremental Tape Recorder, for direct registration of photometric data on computer tape. The computer tape was fed to a UNIVAC 1108 computer which was used for storage of data and for drawing figures on a Kingmatic drawing machine (Kongsberg Våpenfabrikk, Kongsberg, Norway).

The Raman spectra were recorded by a Coderg PH1 spectrometer using a pulsed ruby laser with an exciting line 6943 Å. The optical arrangement and the furnace system have been described in detail previously.[9,10]

Chemicals. To obtain $AlCl_3$ of satisfactory purity, it was made in the laboratory from 99.999 % Al (Vigeland Brug, Vigeland, Norway) and HCl at 450 °C. The HCl was generated from the reaction of *p.a.* H_2SO_4 with *p.a.* NaCl. We obtained $AlCl_3$ of high optical quality, with no light scattering silicon particles after two successive sublimation steps. The following precautions were observed:

(a) Apparatus was scrupulously cleaned;

(b) The quartz was taken to red heat under vacuum at the final stage;

(c) Grease was not used in the teflon and quartz parts of the apparatus.

Water-free $MnCl_2$ was obtained from *p.a.* hydrated $MnCl_2$ (Merck, Darmstadt, Germany) by treatment with HCl, and gradual heating to above the melting point. In the final step, HCl and then high-purity N_2 were bubbled through the $MnCl_2$ melt, which was filtered through a quartz frit and sealed into a quartz ampoule.

CsCl *p.a.* (Analar, Hopkin & Williams Ltd.) was recrystallized in distilled water. The purified crystals were heated under vacuum at 400 °C for 2 h, then heated to above the melting point and filtered through a quartz frit.

Procedure. The anhydrous salts were weighed out in a dry box with water content less than 20 ppm. The salts were added to a quartz tube fitted with a quartz filter and an optical cell. The tube with the cell was transferred to a high-vacuum line and, in the case of the $MnCl_2$-CsCl system, the mixture was melted above the frit and then filtered into the optical cell, which then was sealed off. Due to the high vapour pressure of $AlCl_3$, a slightly different procedure was used for transferring the $MnCl_2$-$AlCl_3$ samples in the cells. The filled tube was first sealed off on the high-vacuum line, well above the frit and the sample. The tube was then placed horisontally in a quartz furnace. When the mixture melted, the furnace was tilted and the melt passed through the filter into the cell under the pressure of aluminium chloride.

All cells were sealed off about 3 cm above the optical zone, in order to have a reservoir where the melt could crystallize. Rupture of the cell by reheating was then prevented by letting the salt crystallize along one wall, not filling any part of the cell completely.

It should be emphazised that the vapour pressure of $AlCl_3$ rises rapidly with temperature in acidic mixtures ($X_{AlCl_3} > 0.5$ in mixtures with monovalent chlorides, $X_{AlCl_3} > 0.66$ in mixtures with divalent chlorides). Such liquids may cause dangerous explosions at elevated temperatures and must be handled behind shields, using appropriate safety measures.

Densities of melts. In order to obtain the concentration in mol/liter and then the molar absorptivities of the spectral transitions, the densities of the samples must be known. The densities of the $MnCl_2$-$AlCl_3$ samples were determined in the optical cell by measuring the height of the melt in the cells with a cathetometer.

RESULTS

Density. The densities (g/cm³) of $MnCl_2$-$AlCl_3$-mixtures at 204 °C in the range 0 to 30 mol % $MnCl_2$ may be represented by the equation:

$$\varrho_{204\,°C}(MnCl_2 - AlCl_3) = 1.208 + 0.934 X_{MnCl_2} + 0.273\, X^{0.5}_{MnCl_2} \quad (2)$$

Standard deviation: 0.009 g/cm³

For the mixture 30 mol % $MnCl_2$ – 70 mol % $AlCl_3$ the temperature dependence in the range

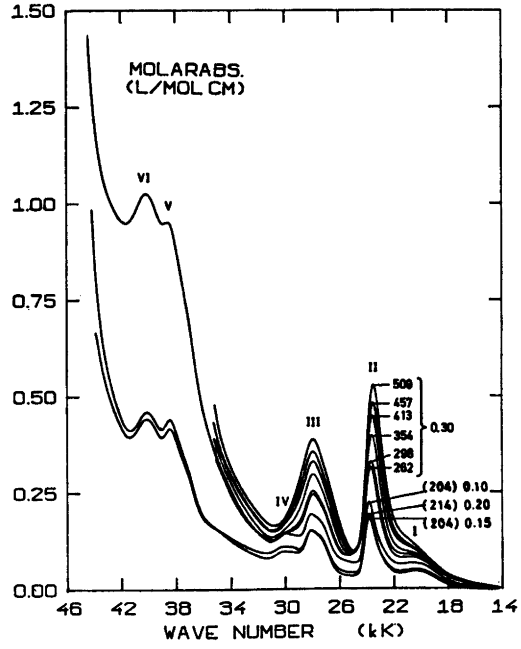

Fig. 1. Absorption spectra of molten $MnCl_2$-$AlCl_3$ mixtures. Temperatures in °C and mol fraction $MnCl_2$ are given.

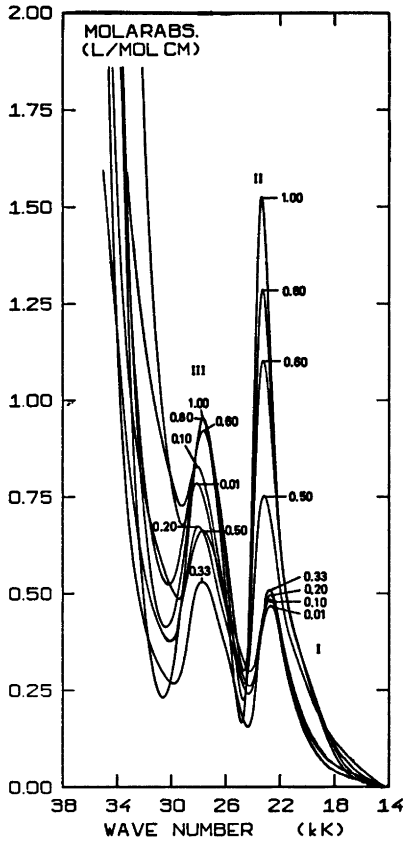

Fig. 2. Absorption spectra of molten $MnCl_2$-CsCl mixtures at 694 °C. Mol fraction $MnCl_2$ is given.

200 °C < t < 500 °C under its own vapour pressure was determined as

$$\varrho(30 \text{ mol \% } MnCl_2 - 70 \text{ mol \% } AlCl_3) = 1.628 - 6.12 \times 10^{-4} \quad (t-200) - 1.99 \times 10^{-7} \quad (t-200)^2 \qquad (3)$$

Standard deviation: 0.002 g/cm³.

The densities of the $MnCl_2$-CsCl mixtures were determined by a hydrostatic weighing method.[11]

Spectra. The absorption spectra of the molten $MnCl_2$-$AlCl_3$ and $MnCl_2$-CsCl mixtures are given in Figs. 1 and 2, and the locations and magnitudes of the absorption maxima are given in Table 1. Assignments of the spectral transitions are also given. The spectra are computer-drawn from tape.

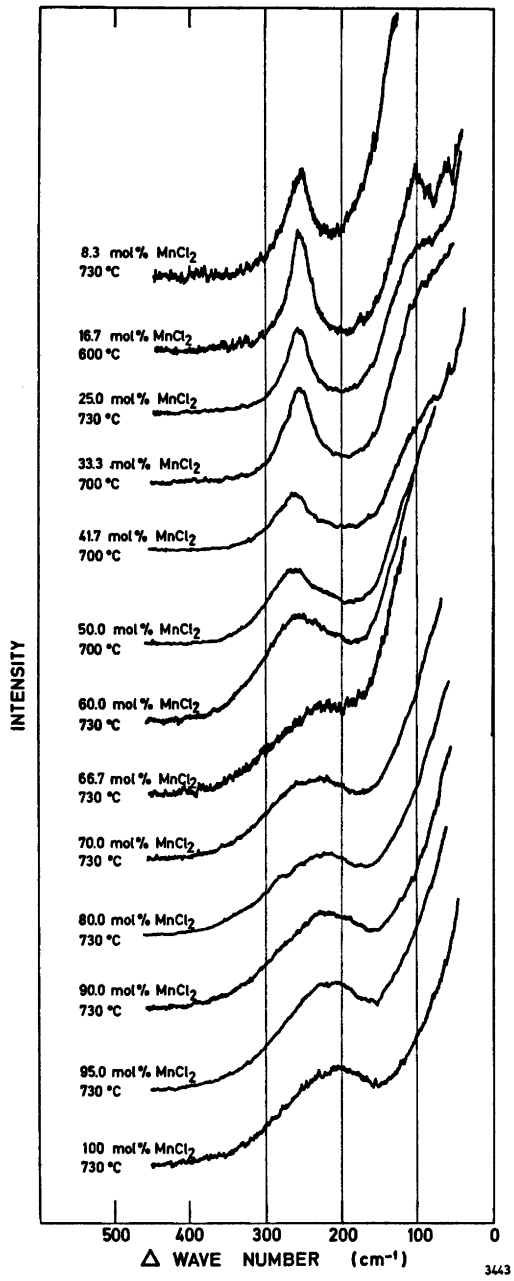

Fig. 3. Raman spectra of molten $MnCl_2$-CsCl mixtures. Optical configuration: Y(X,Y)X.

Figs. 3 and 4 give the Raman spectra of molten $MnCl_2$-CsCl mixtures and of two solid compounds. The spectra were recorded by using

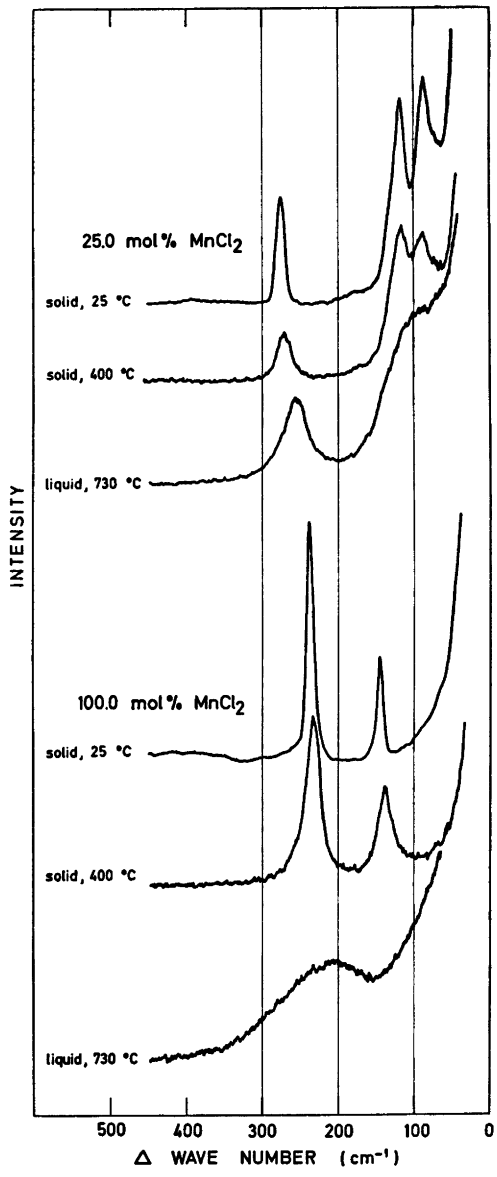

Fig. 4. Raman spectra of the compounds Cs_3MnCl_5 and $MnCl_2$ in the solid and molten state. Optical configuration: Y(X,Y)X.

the optical configuration Y(X,Y)X. Polarization spectra Y(X,Z)X revealed that the strong band observed between 200 and 300 cm^{-1} was polarized. Fig. 5 gives the Raman spectrum of a molten mixture of 25 mol % $MnCl_2$ and 75 mol % $AlCl_3$.

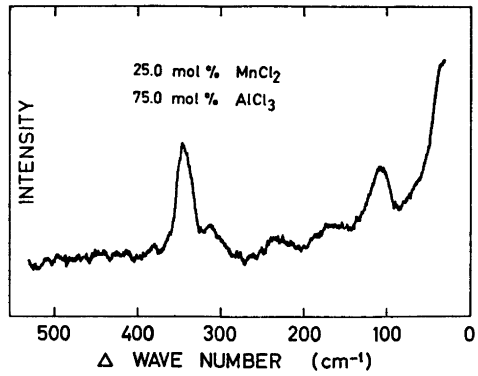

Fig. 5. Raman spectrum of a molten mixture at 250 °C of 25 mol % $MnCl_2$ and 75 mol % $AlCl_3$.

DISCUSSION

The absorption spectra in Fig. 1 can be used to determine the amount of $MnCl_2$ in the $MnCl_2$-$AlCl_3$ mixtures of potential technical importance. The molar absorptivity is approximately concentration independent, and the absorptivity of the peak at 23.8 kK can be used as a measure of the $MnCl_2$ content. The slightly higher absolute intensity value of the 5 and 10 mol % $MnCl_2$-mixture, as compared with 15 and 20 mol %, is probably due to a higher background absorption caused by the use of imperfect optical cells. The 30 mol % $MnCl_2$ mixture had to be recorded at a somewhat higher temperature, but when extrapolated down to 204 °C the spectra are considered to be essentially identical to those of the other compositions.

In spite of carefully recorded absorption and Raman spectra, the structural information obtained is limited. This is partly due to the structural insensitivity of the half-filled *d*-shell of Mn^{2+} and partly due to the fact that Raman spectroscopy mainly gives detailed information when definite species are present. The following structural features can, however, be distinguished.

(a) *Octahedrally coordinated* Mn^{2+}. The absorption spectra of Mn^{2+} in $MnCl_2$-$AlCl_3$ liquid mixtures, $X_{MnCl_2} \leq 0.30$ (Fig. 1), can be attributed to octahedral coordination of Mn^{2+} in accordance with what was previously proposed for a 5 mol % solution of $MnCl_2$ in liquid

Table 1. Electronic transitions in the Mn^{2+} in chloride melts. Ground state: $^6A_{1g}(S)$.

$MnCl_2$ Mol fraction	Temp. °C	Band maxima kK (Molar absorptivity l mol^{-1} cm^{-1})									
$MnCl_2$-$AlCl_3$		I		II		III		IV		V	VI
0.05 [a]	204	20.61	(0.077)	23.85	(0.23)	28.13	(0.22)	30.30	(0.20)	38.78	40.51
0.10	204	20.57	(0.068)	23.84	(0.23)	28.11	(0.20)	30.08	(0.15)	38.55	40.18
0.15	204	20.38	(0.054)	23.85	(0.19)	28.11	(0.16)	30.05	(0.11)	38.47	40.13
0.20	214	20.42	(0.049)	23.85	(0.20)	28.11	(0.16)	30.07	(0.10)	38.45	40.12
0.30	262	20.65sh	(0.083)	23.75	(0.32)	28.02	(0.25)				
0.30	298			23.70	(0.33)	28.00	(0.25)				
0.30	354			23.66	(0.40)	28.00	(0.30)				
0.30	413			23.62	(0.45)	28.02	(0.33)				
0.30	457			23.57	(0.49)	28.01	(0.36)				
0.30	509			23.54	(0.54)	28.00	(0.39)				
$MnCl_2$-CsCl											
1.00	694		≃20 sh	23.30	(1.52)	27.63	(0.95)				
0.80	694		≃20 sh	23.26	(1.29)	27.64	(0.95)				
0.60	694		≃20 sh	23.15	(1.10)	27.58	(0.92)				
0.50	694		≃20 sh	23.05	(0.75)	27.58	(0.66)				
0.33	694		≃20 sh	22.75	(0.51)	27.71	(0.53)				
0.20	694		≃20 sh	22.66	(0.50)	28.00	(0.68)				
0.10	694		≃20 sh	22.66	(0.49)	28.09	(0.83)				
0.01	694		≃20 sh	22.64	(0.47)	28.10	(0.79)				

Assignment of upper energy level. Transitions observed as shoulders given in [ ]	$^4T_{1g}(G)$	$[^4T_{2g}(G)]$ $^4E_g\,^4A_{1g}(G)$	$[^4T_{2g}(D)]$ $^4E_g(D)$	$^4T_{1g}(P)$	$^4A_{2g}(F)$ $^4T_{1g}(F)$	$^4T_{2g}(F)$
Octahedral Mn^{2+}, values in kK.[13]	19.30	[22.70] 23.88	[27.20] 28.14	30.02	38.50	42.70
Tetrahedral Mn^{2+}, values in kK.[14]	21.20	[22.40] 23.20	[26.30] 27.10	27.90	~38.00 38.30 [b]	39.30 [b]

[a] Taken from chart and not given in Fig. 1 as the computer tape got destroyed. [b] Calculated.

$AlCl_3$.[12] Except for some deviation for the first $^4T_{1g}(G) \leftarrow {}^6A_{1g}(S)$ transition, the transitions correspond very closely to those determined by Mehra and Venkateswarlu,[13] based on the experimental spectra of Mn^{2+} in a KCl host lattice with five transitions appearing as peaks and two as shoulders (Table 1). The increased band intensity with increasing temperature, accompanied by an increased molar absorptivity of the low energy band side, are consistent with a vibronic mechanism generally operative for an octahedral centrosymmetric ligand field.[15]

The spectra of Fig. 1 demonstrate that the environment around Mn^{2+} is invariant in the measured range 0 – 30 mol % $MnCl_2$. Severe structural changes do, however, occur for compositions somewhat above 30 mol % $MnCl_2$, manifested by a steep rise of the melting point.[16]

Previous Raman studies have shown the following species to be present as the acidity is increased: $AlCl_4^-$, $Al_2Cl_7^-$, possibly $Al_3Cl_{10}^-$, Al_2Cl_6.[2,5,17] $Al_2Cl_7^-$ is a double tetrahedron with a Cl-bridge.

The acid-base reaction can be written as shown in eqns. (4) and (5):

$$2Al_2Cl_6 + MnCl_2 = 2Al_2Cl_7^- + Mn^{2+} \quad (4)$$

$$Al_2Cl_6 + MnCl_2 = 2AlCl_4^- + Mn^{2+} \quad (5)$$

If the equilibria (4) and (5) are shifted completely to the right, $AlCl_3$ becomes saturated as $AlCl_4^-$ when the $MnCl_2$ content is above 33 mol %, corresponding to the stoichiometry $Mn(AlCl_4)_2$, and further addition of $MnCl_2$ does not result in an acid-base reaction. It would have been of great interest to follow the structural changes around 33 mol % spectroscopically, but repeated explosions of the cells, due to high temperatures and pressures, prevented this, In the studied melts Mn^{2+} is considered coordinated octahedrally to $AlCl_4^-$ or $Al_2Cl_7^-$ forming strong ionic bonds.[18]

The Raman spectra of $MnCl_2$-$AlCl_3$ mixtures were recorded in order to obtain additional information. The spectra proved generally to be of rather poor quality, and only the best spectrum is shown in Fig. 5, for a mixture containing 25 mol % $MnCl_2$ and 75 mol % $AlCl_3$.

The spectrum is interpreted as follows: A strong peak at 344 cm^{-1} due to Al – Cl stretch in $AlCl_4^-$ and Al_2Cl_6 groupings,[2] a weak peak at 311 cm^{-1} due to Al – Cl stretch in $Al_2Cl_7^-$ groupings,[2] a broad band at 233 cm^{-1} probably due to Mn – Cl stretch for Mn^{2+} in octahedral positions, and two broad depolarized bands at 169 and 105 cm^{-1} due to Mn – Cl and Al – Cl bending modes.[2]

With Mn^{2+} having higher charge over radius ratio than the alkali ions, the $Al_2Cl_7^-$ seems to be destabilized relative to what is observed in $AlCl_3$-alkali chloride mixtures.[5] The spectra do not contradict the model of Mn^{2+} coordinated octahedrally to $AlCl_4^-$ and $Al_2Cl_7^-$ groupings, but overlaps of bands due to $AlCl_4^-$ and Al_2Cl_6 [5] and the relative poor spectral quality do prevent a detailed discussion of the structure.

(b) *Tetrahedral $MnCl_4^{2-}$ species.* Although $MnCl_2$ is a base towards $AlCl_3$ it can act as an acid towards CsCl, according to eqn. (6):

$$MnCl_2 + 2CsCl = MnCl_4^{2-} + 2Cs^+ \qquad (6)$$

If we assume this system is analogous to the $AlCl_3$-$MnCl_2$ acid-base system with the equilibrium shifted to the right, reaction (6) will be completed when the content of CsCl becomes higher than 66 mol%, corresponding to the stoichiometry of Cs_2MnCl_4. For stoichiometric reasons $MnCl_4^{2-}$ exists as separate tetrahedral units *only*, above 66 mol % CsCl.

The Raman spectra (Figs. 3 and 4) give strong support for the assumption of formation of separate tetrahedral $MnCl_4^{2-}$ units in mixtures of $MnCl_2$ with excess CsCl. In Fig. 4 the three upper curves show the spectra of solid Cs_3MnCl_5 where separate $MnCl_4^{2-}$ groupings are present,[19,20] compared with the spectra of the compound in the molten state. Taking into consideration the observed shift to lower frequencies with temperature and some broadening of peaks in the molten state, a close resemblance between the spectra of the solid and the liquid is demonstrated. Not only the symmetric stretching mode A_1 at 255 cm^{-1}, but also the E and one of the F_2 modes in the region 130 – 70 cm^{-1} are apparent.

The absorption spectra of $MnCl_2$ with CsCl in the concentration range $0 < X_{MnCl_2} \leq 0.33$ (Fig. 2) differ from that of $MnCl_2$ in $AlCl_3$ (Fig. 1), but the spectra in mixtures with CsCl are less structured and ligand field spectroscopy gives little aid in characterizing Mn^{2+} as $MnCl_4^{2-}$. This is more so as the spectra of octahedral [13] and tetrahedral [14] coordination can be very similar (Table 1).

However, we conclude, based on Raman spectra evidence, that $MnCl_4^{2-}$ is the major species in molten $MnCl_2$-CsCl mixtures with excess CsCl. The species $MnCl_4^{2-}$ has also previously been suggested from absorption spectroscopy,[21] from calorimetry [22] and very recently from Raman spectroscopy.[23]

(c) *Structural changes in liquid $MnCl_2$-CsCl mixtures.* To clarify the structural changes in molten $MnCl_2$-CsCl mixtures, we have plotted the location of the two bands that changes most significantly with composition, namely the maximum of the absorption band II (Fig. 2) and the maximum of the Raman symmetric stretching mode (Fig. 3) (Fig. 6).

The observed Raman shifts are qualitatively parallel to those observed in $MnCl_2$ – KCl by Tanemoto and Nakamura,[23] and also to what is observed for $ZnCl_2$-alkali chloride systems.[24–27]

Additional support for the existence of separate $MnCl_4^{2-}$ units in the range $0 < X_{MnCl_2} \leq 0.3$ is inferred from the graphs in Fig. 6 as the spectra remain unchanged in this region. In fact the shift of the symmetric stretching frequency begins around $X_{MnCl_2} = 0.33$, where this model starts to be untenable.

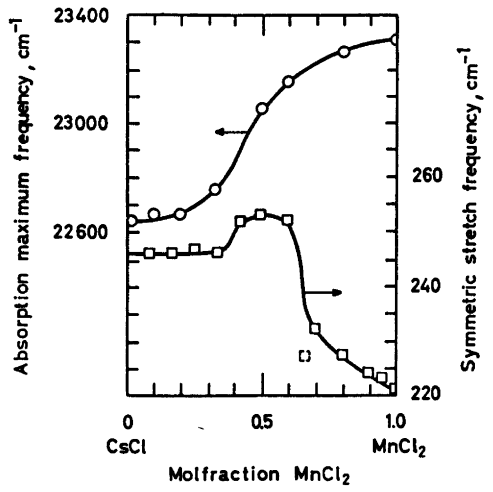

Fig. 6. Band shifts in molten $MnCl_2$-CsCl mixture with composition. ○, Maximum of absorption band II (Fig. 2, Table 1); □, maximum of the Raman symmetric stretching frequency (Fig. 3).

As an increase in coordination number generally leads to a lowering of the symmetric stretching frequency, see for instance Ferraro [28] who gives empirical rules, the following coordination changes could be expected:

$0 < X_{MnCl_2} < 0.33$: $MnCl_4^{2-}$ units

$0.33 < X_{MnCl_2} < 0.50$: $MnCl_4^{2-}$ units→$MnCl_3^-$ units

$0.50 < X_{MnCl_2}$: $MnCl_3^-$ units→octahedral coordination in lattice-like structure with Cl-bridging.

This model, however, does not explain readily the S-shaped shift of the location of the absorption band (Fig. 6) and the increased molar absorptivity with increasing $MnCl_2$-content (Fig. 2).

An alternate model which in a better way incorporates the absorption spectroscopic results as well, considers the structural changes due to increased Cl-bridging without change of coordination number:

Mainly tetrahedral coordination for all compositions.

$0 < X_{MnCl_2} < 0.33$: $MnCl_4^{2-}$ units

$0.33 < X_{MnCl_2} < 0.50$: Linear bridging ($MnCl_4^{2-}$→$Mn_2Cl_7^{3-}$→$Mn_nCl_{3n+1}^{-(n+1)}$)

$0.50 < X_{MnCl_2}$: Transformation from linear to three-dimensional bridging.

The experimentally observed lowering of the stretching frequency for $X_{MnCl_2} > 0.6$ is then understood as the effect of three-dimensional bridging retaining the tetrahedral coordination. Linear bridging may, however, not necessarily give a decreased stretching frequency, and the increased stretching frequency for $0.33 < X_{MnCl_2} < 0.6$ can be explained by the presence of linear polymers. An experimental verification of this point is found by comparison with a similar system: $GaCl_4^-$-$Ga_2Cl_7^-$. For these ions the central atom is heavier than Cl (as in the case of Mn), and the totally symmetric stretching frequency is shifted from 342 cm^{-1} for $GaCl_4^-$ to 366 cm^{-1} for $Ga_2Cl_7^-$.[10]

The strong shift in the location of the absorption maximum for $0.33 < X_{MnCl_2} < 0.5$ may then be correlated with a change in the ligand field accompanied by increased linear polymerization. It is also easier to understand the increase in molar absorptivity with increasing content of $MnCl_2$ (Fig. 2), as due to some distortion of the tetrahedral coordination connected with the three-dimensional bridging rather than transformation to an octahedral coordination where decrease in molar absorptivity generally is expected. This model is suggested in spite of the similarity of the Raman spectra of molten $MnCl_2$ and solid $MnCl_2$ where Mn^{2+} is octahedrally coordinated (Fig. 4).

The low viscosity of pure molten $MnCl_2$ indicates that a three-dimensional bridging may be less complete than in SiO_2 or $ZnCl_2$.

In conclusion we would point to the qualitative difference of the Raman spectra in $MnCl_2$—CsCl mixtures above and below 33 mol % $MnCl_2$ (Fig. 3). The peaks are relatively sharp below 33 mol % $MnCl_2$, pointing to isolated $MnCl_4^{2-}$ tetrahedra being the dominating species, while the broadness above 33 mol % probably is a result of several overlapping peaks due to a much more disordered structure.

Acknowledgement. We express our gratitude to The Norwegian Agency for International Development which, by a grant to one of us (Laila El-Sayed), made this work possible. We also gratefully acknowledge the experimental assistance of Mr. Morten Sørlie, and "Norges almenvitenskapelige forskningsråd"

for financial support. Mr. D. Grünewald ably assisted with the Raman spectrometer, being financed by a grant from "Die Volkswagenstiftung". Discussions with Dr. M. H. Brooker are also gratefully acknowledged.

REFERENCES

1. Cyvin, S. J., Klæboe, P., Rytter, E. and Øye, H. A. *J. Chem. Phys. 52* (1970) 2776.
2. Øye, H. A., Rytter, E., Klæboe, P. and Cyvin, S. J. *Acta Chem. Scand. 25* (1971) 559.
3. Kvaal, T. and Øye, H. A. *Acta Chem. Scand. 26* (1972) 1647.
4. Øye, H. A. and Bues, W. *Inorg. Nucl. Chem. Lett. 8.* (1972) 31.
5. Rytter, E., Øye, H. A., Cyvin, S. J., Cyvin, B. N. and Klæboe, P. *J. Inorg. Nucl. Chem. 35* (1973) 1185.
6. Applied Aluminium Research Corporation: Presentation of the Toth Aluminium Production Process 1973, New Orleans, USA.
7. Grjotheim, K., Krohn, C. and Øye, H. A. *Aluminium 51* (1975) 697.
8. Borgen, O. and Bruvoll, T., *Technical Report 70*, Institutt for fysikalsk kjemi, Norges tekniske høgskole, Universitetet i Trondheim, Trondheim 1974.
9. Bues, W., Brockner, W. and Grünewald, D. *Spectrochim. Acta A 28* (1972) 1519.
10. Øye, H. A. and Bues, W. *Acta Chem. Scand. A 29* (1975) 489.
11. El-Sayed, L. and Øye, H. A. *Acta Chem. Scand. A 29* (1975) 267.
12. Øye, H. A. and Gruen, D. M. *Inorg. Chem. 3* (1964) 836.
13. Mehra, A. and Venkateswarlu, P. *J. Chem. Phys 45* (1966) 3381.
14. Cotton, F. A., Goodgame, D. M. L. and Goodgame, M. *J. Am. Chem. Soc. 84* (1962) 167.
15. Ferguson, J. *Progr. Inorg. Chem. 12* (1970) 159.
16. Levin, E. M., Robbins, C. R. and McMurdie, H. F. *Phase Diagrams for Ceramists 1969 Supplement*, The American Ceramic Soc., Columbus, Ohio 1969.
17. Rytter, E. *Thesis*, No. 26, Institutt for uorganisk kjemi, Norges tekniske høgskole, Universitetet i Trondheim, Trondheim 1974.
18. Anundskås, A. and Øye, H. A. *J. Inorg. Nucl. Chem. 37* (1975) 1609.
19. Andersen, P. *Resymé*, 9. Nordiske kemikermøde, Aarhus 1956, p. 7.
20. Goodyear, J. and Kennedy, D. J. *Acta Cryst. B 32* (1976) 631.
21. Sundheim, B. R. and Kukk, M. *Discuss. Faraday Soc. 32* (1961) 49.
22. Papatheodorou, G. N. and Kleppa, O. J. *Inorg. Nucl. Chem. 33* (1971) 1249.
23. Tanemoto, K. and Nakamura, T. *Chem. Lett. Jpn.* (1975) 351.
24. Bues, W. *Z. Anorg. Allg. Chem. 152* (1955) 104.
25. Moyer, J. R., Evans, J. C. and Lo, G. Y.-S. *J. Electrochem. Soc. 113* (1966) 158.
26. Ellis, R. B. *J. Electrochem. Soc. 113* (1966) 485.
27. Bues, W. and Brockner, W. *Z. Phys. Chem. N. F. 88* (1974) 290.
28. Ferraro, J. R. *Low-Frequency Vibrations of Inorganic and Coordination Compounds*, Plenum, New York 1971, Chapter 6.

Received January 28, 1977.